ORIGINAL ARTICLE

Apoptotic blebs from leukemic cells as a preferred source of tumor-associated antigen for dendritic cell-based vaccines

Jurjen M. Ruben · Willemijn van den Ancker · Hetty J. Bontkes ·
Theresia M. Westers · Erik Hooijberg · Gert J. Ossenkoppele ·
Tanja D. de Gruijl · Arjan A. van de Loosdrecht

Abstract Since few leukemia-associated antigens (LAA) are characterized for acute myeloid leukemia (AML), apoptotic tumor cells constitute an attractive LAA source for DC-based vaccines, as they contain both characterized and unknown LAA. However, loading DC with apoptotic tumor cells may interfere with DC function. Previously, it was shown in mice that apoptotic blebs induce DC maturation, whereas apoptotic cell remnants (ACR) do not. Here, we analyzed human monocyte-derived DC (MoDC) functionality in vitro, after ingesting either allogeneic AML-derived ACR or blebs. We show that MoDC ingest blebs to a higher extent and are superior in migrating toward CCL19, as compared to ACR-loaded MoDC. Although MoDC cytokine production was unaffected, co-culturing bleb-loaded MoDC with T cells led to an increased T cell proliferation and IFNγ production. Moreover, antigen-specific CD8$^+$ T cells frequencies increased to 0.63 % by priming with bleb-loaded MoDC, compared to 0.16 % when primed with ACR-loaded MoDC. Importantly, CD8$^+$ T cells primed by bleb-loaded MoDC recognized their specific epitope at one to two orders of magnitude lower concentrations compared to ACR-loaded MoDC. In conclusion, superior ingestion efficiency and migration, combined with favorable T cell cytokine release and CD8$^+$ T cell priming ability and avidity, point to blebs as the preferred component of apoptotic leukemic cells for LAA loading of DC for the immunotherapy of AML.

J. M. Ruben (✉) · W. van den Ancker · H. J. Bontkes ·
T. M. Westers · G. J. Ossenkoppele ·
A. A. van de Loosdrecht (✉)
Department of Hematology, Cancer Center Amsterdam,
VU University Medical Center, De Boelelaan 1117,
1081 HV Amsterdam, The Netherlands

A. A. van de Loosdrecht
e-mail: a.vandeloosdrecht@vumc.nl

E. Hooijberg
Department of Pathology, Cancer Center Amsterdam,
VU University Medical Center, De Boelelaan 1117,
1081 HV Amsterdam, The Netherlands

T. D. de Gruijl
Department of Medical Oncology, Cancer Center Amsterdam,
VU University Medical Center, De Boelelaan 1117,
1081 HV Amsterdam, The Netherlands

Introduction

Dendritic cells (DC) have the ability to ingest and process exogenous proteins and to present derived peptides thereof at the cell surface in complex with HLA class II molecules, or via cross-presentation in the context of HLA class I molecules. DC can potentiate antigen-specific T cell responses and are therefore of major interest as mediators of anti-tumor immunity in vaccination strategies [1, 2]. In order to induce tumor-specific immune responses, DC are required to present tumor-associated antigen(s) (TAA). Next to the generation of DC from chronic and acute myeloid leukemia (CML and AML, respectively) cells [3, 4], multiple strategies for loading DC with TAA have been investigated, such as peptide pulsing [5, 6], TAA-specific mRNA electroporation [7–9], and loading of necrotic or apoptotic tumor cells via phagocytosis [4, 5, 10, 11]. Thus far, the focus has been

on targeting solid tumors (mostly melanoma), but DC vaccination is a potential therapy for treating AML patients in a minimal residual disease setting as well. Recently, a small-scale phase I clinical study demonstrated vaccination of elderly AML patients with autologous AML blast cell-loaded monocyte-derived DC (MoDC) to be safe and to induce (transient) disease stabilization and specific CD8^{+} T cells [12]. The use of leukemic blasts as a source of leukemia-associated antigen (LAA) for DC loading is particularly attractive, as they contain both characterized and as yet unidentified LAA and, moreover, pave the way to generate tumor- and patient-specific vaccines. However, loading DC with apoptotic blasts could impair DC function, due to the immunosuppressive nature of apoptotic cells [13–18].

Apoptotic cells undergo multiple macro- and microcellular rearrangements, e.g., cellular condensation, pyknosis, karyorrhexis, redistribution of specific organelles into peripheral membrane protrusions (blebbing), and the exposure of apoptosis-specific structures on the cell membrane, e.g., phosphatidyl serine, calreticulin as well as alterations in the glycocalyx that act as "eat-me" signals for phagocytes [19–22]. During the blebbing phase mainly the endoplasmic reticulum (ER), RNA and chromatin are enclosed in blebs, which become detached from the main apoptotic cell at later stages of apoptosis [21, 23]. Although the exact functional relevance of blebbing during apoptosis remains elusive, it was shown that ingestion of blebs by mouse bone marrow-derived DC (BMDC) induced DC maturation and subsequent T helper-17 cell activation when co-cultured with splenocytes in vitro, whereas the remaining apoptotic cell remnants (ACR) did not [30, 31]. Of note, there is some confusion in the literature regarding the use of the term apoptotic bodies, which is at times used to describe both ACR and blebs [23, 24]. Although multiple studies have analyzed the effect of loading apoptotic cells or apoptotic bodies (ACR) on DC, no studies have been conducted thus far which analyzed the selective use of apoptotic blebs (microvesicles that require additional isolation steps) as a source of TAA for human DC loading. Since blebs have been shown to activate BMDC in mice [23] and in view of a growing recognition of the need to utilize the unique mutanome of individual tumors for vaccination strategies, DC loaded with AML blast-derived blebs may constitute an effective vaccine. Here, we compared MoDC phenotype and function in vitro, after ingestion of either ACR or blebs derived from a human AML cell line.

Materials and methods

Cell lines

The human HLA-A2-negative AML cell line HL60 (ATCC, Wesel, Germany) was cultured in RPMI containing 10 %

FCS, 100 IU/ml penicillin, and 100 μg/ml streptomycin (all Gibco, Paisley, UK), further referred to as complete medium.

Generation of MoDC

Peripheral blood mononuclear cells (PBMCs) were isolated from buffy coats of healthy volunteers by centrifugation on a Ficoll–Paque density gradient medium, after informed consent. Subsequently, monocytes were isolated from PBMCs by positive selection using magnetic activated cell sorting with CD14 microbeads (Miltenyi biotec, Utrecht, the Netherlands). MoDC were generated by culturing monocytes for 5 days at 37 °C in complete medium, in the presence of 800 U/ml GM-CSF (1×10^7 U/mg, Peprotech, the Netherlands) and 500 U/ml IL-4 (5×10^6 U/mg, Peprotech, the Netherlands). After 5 days of culture, MoDC were either used directly or stored in liquid nitrogen until further use. One hour after loading MoDC with ACR or blebs, maturation was induced by a cytokine cocktail consisting of IL-1β (10 ng/ml, 1×10^9 U/mg, Sanquin, Amsterdam, the Netherlands), IL-6 (10 ng/ml, 2×10^6 U/mg, R&D systems, Abingdon, UK), TNFα (200 U/ml, 2×10^7 U/mg, Sanquin, Amsterdam, the Netherlands), and PGE2 (10 ng/ml, Sigma-Aldrich, Zwijndrecht, the Netherlands).

Preparation of apoptotic cell fractions

Apoptosis of HL60 cells was induced by adding 3 μM mitoxantrone dihydrochloride (mitoxantrone; Sigma-Aldrich, Zwijndrecht, the Netherlands) per 2×10^6 HL60 cells per ml of complete medium, for 48 h at 37 °C, 5 % CO_2. We were unable to perform priming experiments with MoDC loaded with either ACR or blebs from mitoxantrone-induced apoptotic HL60 cells, since T cells did not expand or underwent apoptosis during co-culture (data not shown). This is likely to be the result of leaked mitoxantrone from the loaded MoDC. We therefore alternatively induced apoptosis of HL60 cells by heat shock (HS), as described before [11]. In short, cells were washed with RPMI 1640 and resuspended at 5×10^6 cells/ml in RPMI 1640 and subsequently incubated for 2 h at 42 °C. Next, the cells were irradiated at 5,000 rad, washed, resuspended at 2×10^6 per ml in full medium, and incubated for 48–72 h at 37 °C, 5 % CO_2. The percentage of apoptotic cells was determined by Syto16 labeling (Molecular Probes, Leiden, the Netherlands). In short, 50×10^3 cells were resuspended in 1 ml PBS, containing 10 % FCS (Greiner Bio-One, Alphen a/d Rijn, the Netherlands), 20 mM HEPES (Sigma-Aldrich), 1 ml/ml glucose anhydrous (Baker B.V. Deventer, the Netherlands), 4 mM L-glutamine (Invitrogen), MEM amino acids (Sigma-Aldrich). Syto16 (42 nM) and the PgP pump inhibitor PSC833 (5 μM; a kind gift from Novartis,

Basel, Switzerland) were added, and the cells were incubated for 30 min at 37 °C, 5 % CO_2 and washed with an excess of PBS. The subsequent caspase-dependent loss of syto16 labeling was analyzed on a BD FACSCanto™ II flow cytometer (BD Biosciences), to assess the level of apoptosis. In all cases, >90 % of the cells was apoptotic [25]. ACR and blebs were isolated by differential centrifugation. The centrifugal force for separating ACR and blebs was determined by assessing the size and appearance of the separated fractions by a Zeiss Axioskop 50 fluorescence microscope (Zeiss, the Netherlands) and a CM100 BioTwin electron microscope (Philips, the Netherlands). ACR were isolated by centrifugation at $600 \times g$ at 4 °C for 10 min, after which the apoptotic blebs were isolated from the resulting supernatant by centrifugation at $4,000 \times g$ at 4 °C for 10 min. Apoptotic fractions were washed twice with excess PBS prior to determining the protein concentration. Apoptotic cell material was lysed by 5 cycles of snap-freezing in liquid nitrogen, followed by thawing in a water bath at 37 °C. Subsequently, cellular material was lysed by 5 cycles of sonication (5 s pulse, followed by 5 s rest) at 18 micron (Sanyo MSE Soniprep 150, Amsterdam, the Netherlands) in the presence of a protease inhibitor cocktail, following the manufacturers' protocol (Complete Mini Protease Inhibitor Cocktail Tablets, Roche Diagnostics, Almere, the Netherlands). Subsequently, the protein concentration was determined by analyzing the absorption at 280/260 nm from 50 µl of lysed samples, using a ND-1000 Nanodrop spectrophotometer (Thermo Fisher Scientific, Breda, the Netherlands). ACR and blebs were either used directly or frozen in liquid nitrogen and thawed prior to usage.

Uptake and internalization of ACR and blebs by- and immuno-phenotyping of MoDC

Prior to inducing apoptosis, HL60 cells were labeled with 1 µM carboxyfluorescein succinimidyl ester (CFSE; Invitrogen, Breda, the Netherlands) and Hoechst 33342 1 µg/ml (Molecular Probes, Eugene, OR, USA) for fluorescence microscopic imaging and MoDC were labeled with 1 µM CellVue Plum (eBioscience, Vienna, Austria). Analysis of the ingestion of apoptotic material by MoDC was analyzed by flow cytometry using a BD FACSCanto™ II flow cytometer and BD FACSDiva™ software.

Internalization of the apoptotic fractions was visualized using confocal microscopy. Thawed ACR and blebs were labeled with 1 µM PKH26 red fluorescent cell linker kit (Sigma-Aldrich), following the manufacturer's protocol. MoDC were labeled with 2 µM CFSE and co-cultured with PKH26-labeled ACR or blebs for 8 h. Loaded MoDC were harvested and washed and transferred to 4 wells Lab-Tek™ Permanox Chamber Slides (Thermo Scientific, the

Netherlands). After overnight adherence, the supernatant was carefully removed and the loaded MoDC were fixed using 1 % paraformaldehyde solution for 15 min at 4 °C, washed with PBS and dried. Vectashield (Vector Laboratories, United Kingdom) was added on the slides, which were covered by a coverslip and analyzed using a Leica TCS SP2 confocal microscope (Leica Microsystems, the Netherlands).

MoDC phenotype was determined by flow cytometric analysis 48 h after loading the apoptotic material, using fluorochrome-conjugated antibodies CD1a, CD54 (Dako Cytomation), CD14, CD80, CD86, CD209 (BD Biosciences), CD40, CD83 (Beckman Coulter), and the unlabeled CCR7 antibody (BD Biosciences) followed by PE-conjugated goat anti-mouse IgM (Beckman Coulter).

Transwell migration assay

Migratory capacity of MoDC after ingesting apoptotic material was analyzed using a transwell migration assay, using membranes with a 5 µM pore size (Corning). Specific versus non-specific migration of 1×10^5 MoDC (deposited in the upper compartment) was determined by performing the transwell migration assay in the presence or absence of 250 ng/ml MIP-3β (added to the lower compartment, CCL19, R&D systems, Abingdon, UK). After 5 h, the number of migrated viable MoDC was quantified using FlowCount™ beads (Dako, Enschede, the Netherlands) on a BD FACSCanto™ II flow cytometer.

MoDC cytokine release

4×10^4 (loaded) MoDC were cultured overnight with 4×10^4 CD40-ligand expressing J558 cells (irradiated at 50 Gy) [26] in the presence of 1,000 U/ml IFNγ (Sanquin, Amsterdam, the Netherlands) in a 96-wells plate. Next, the plates were spun at $1,000 \times g$, and the supernatants were directly analyzed for the presence of cytokines using an inflammatory cytokine bead array (BD Biosciences, Breda, the Netherlands), following the manufacturer's protocol.

Mixed lymphocyte reaction and cytokine release

Peripheral blood lymphocytes (PBL) from healthy donors were labeled with 1 µM CFSE and subsequently co-cultured with allogeneic (loaded) MoDC for 6 days, after which the cells were harvested and labeled with CD3, CD4, and CD8 (BD biosciences), and the CFSE dilution over the daughter $CD3^+CD4^+$ and $CD3^+CD8^+$ T cells was measured using flow cytometry (BD FACSCanto™ II) and analyzed using BD FACSDiva™ software. Moreover, supernatants were harvested for cytokine analysis using a T_H1/

T_H2/T_H17 cytokine bead array (BD Biosciences, Breda, the Netherlands), following the manufacturers' protocol.

CD8$^+$ T cell priming and avidity analysis

Autologous in vitro T cell priming experiments were conducted as described previously [27]. In order to analyze MART-1-specific CD8$^+$ T cell outgrowth, we generated a MART-1 expressing HL60 cell line (as well as a K562 cell line, referred to as K562-M, as a (HLA-A2) negative control for the analysis of cytotoxicity) by retroviral transduction of LZRS-MART-1-IRES-ΔNGFR, as reported previously [28].

MoDC were loaded overnight with MART-1-positive ACR or blebs and matured as described above, co-cultured with autologous thawed CD8$^+$ T cells and irradiated CD14$^-$/CD8$^-$ PBL, and restimulated with loaded MoDC after 10 days and subsequently every 7 days. The HLA-A2-restricted expansion of MART-1$_{26-35L}$ CD8$^+$ T cells was analyzed in each well by tetramer staining, using flow cytometry (LSRFortessa™, BD Biosciences). Next, MART-1$_{26-35L}$ tetramer-positive CD3$^+$/CD8$^+$ T cells were sorted using a BD FACSAria III cell sorter (BD Biosciences) and polyclonally expanded. The CD8$^+$ T cell avidity was assessed by co-culture with loaded JY cells (concentrations ranging from 10 μM to 100 fM), by an intracellular IFNγ readout (BD Biosciences).

Cytotoxicity assay

Cytotoxicity was determined by co-culturing primed and sorted CD8$^+$ T cells [labeled with 50 nM CFSE (Invitrogen)], at effector-to-target ratios starting from 0:1 to 10:1, with 200 nM CellVue (eBiosciences) labeled melanoma Mel AKR cells (HLA-A2-positive and MART-1-positive; the Netherlands Cancer Institute, Amsterdam, the Netherlands), JY cells (HLA-A2-positive, MART-1-negative), or K562-M (HLA-A2-negative and MART-1-positive). After an overnight co-culture, target cells were shortly (<5 min) incubated with 50 μl 0.05 % Trypsin–EDTA solution (Invitrogen), suspended by careful tapping and washed with 150 μl complete medium. Next, the cells were resuspended in a 2 % BD Via-Probe/PBS/0.1 %human serum albumin solution, incubated for 10 min, and the percentage of BD Via-Probe-positive CellVue$^+$/CFSE$^-$ target cells was measured using flow cytometry (LSRFortessa™, BD Biosciences).

Statistical analysis

Statistical analysis was performed in GraphPad Prism version 5 for Windows (GraphPad Software Inc.,), using a paired two-tailed Student t test. p values ≤0.05 were regarded as significant.

Results

ACR and blebs isolated from HL60 AML cells represent distinct cellular components

After isolation of ACR and blebs from mitoxantrone treated apoptotic HL60 cells, we analyzed their morphological appearance and size, using transmission electron microscopic imaging (Fig. 1a, b). ACR appeared as a heterogeneous population of large cellular bodies of approximately 2–10 μm in size with a ruffled plasma membrane that appeared to be locally disintegrated (Fig. 1a, arrows). Electron dense areas resided within the ACR (Fig. 1a, asterisk) that were enclosed by a membrane and represent the latest stages of chromatin translocation to the periphery of the cell, which was confirmed by fluorescence microscopy after the labeling of proteins (CFSE) and DNA (Hoechst 33342) in apoptotic ACR (Fig. 1c).

Apoptotic blebs are described as 100–1,000 nM microvesicles, containing both chromatin and ER. Both cellular components are actively translocated from the apoptotic cell into peripheral vesicles during apoptosis and become enclosed by a sheet of ER membrane and a sheet of plasma membrane [21, 29]. The isolated fraction contained a heterogeneous population of blebs 200–600 nM in diameter (Fig. 1b). They were indeed enclosed by a characteristic double membrane, as described previously [21], and as shown in Fig. 1b, open arrows. Moreover, characteristic structures resembling ER and ribosomes were also observed (Fig. 1b, closed arrows). Using electron microscopic imaging, we could not detect blebs containing electron dense areas (chromatin). Fluorescent imaging showed few blebs to stain positive for Hoechst 33342 (Fig. 1d).

Blebs are ingested by a higher percentage of MoDC than ACR

We analyzed whether MoDC were able to internalize both mitoxantrone-induced ACR and blebs, by co-culturing CFSE-labeled MoDC with PKH26-labeled apoptotic material. Indeed, analysis using confocal microscopy demonstrated that both ACR (Fig. 2a, upper panel) and blebs (Fig. 2a, lower panel) could be internalized by MoDC. Next, we quantified the ingestion of ACR or blebs using flow cytometry (Fig. 2b), by co-culturing MoDC overnight with either CFSE-labeled ACR or blebs. During co-culture, MoDC did not receive any additional maturation stimuli (further referred to as immature DC) or received a maturation inducing cocktail 1 h after initiation of the co-culture, consisting of the cytokine cocktail IL-1β, IL-6, PGE-2, and TNF-α (further referred to as maturing DC). Blebs were ingested by 70 % (mean, range 41–95 %) of the immature MoDC, whereas ACR were ingested by 46 % (mean,
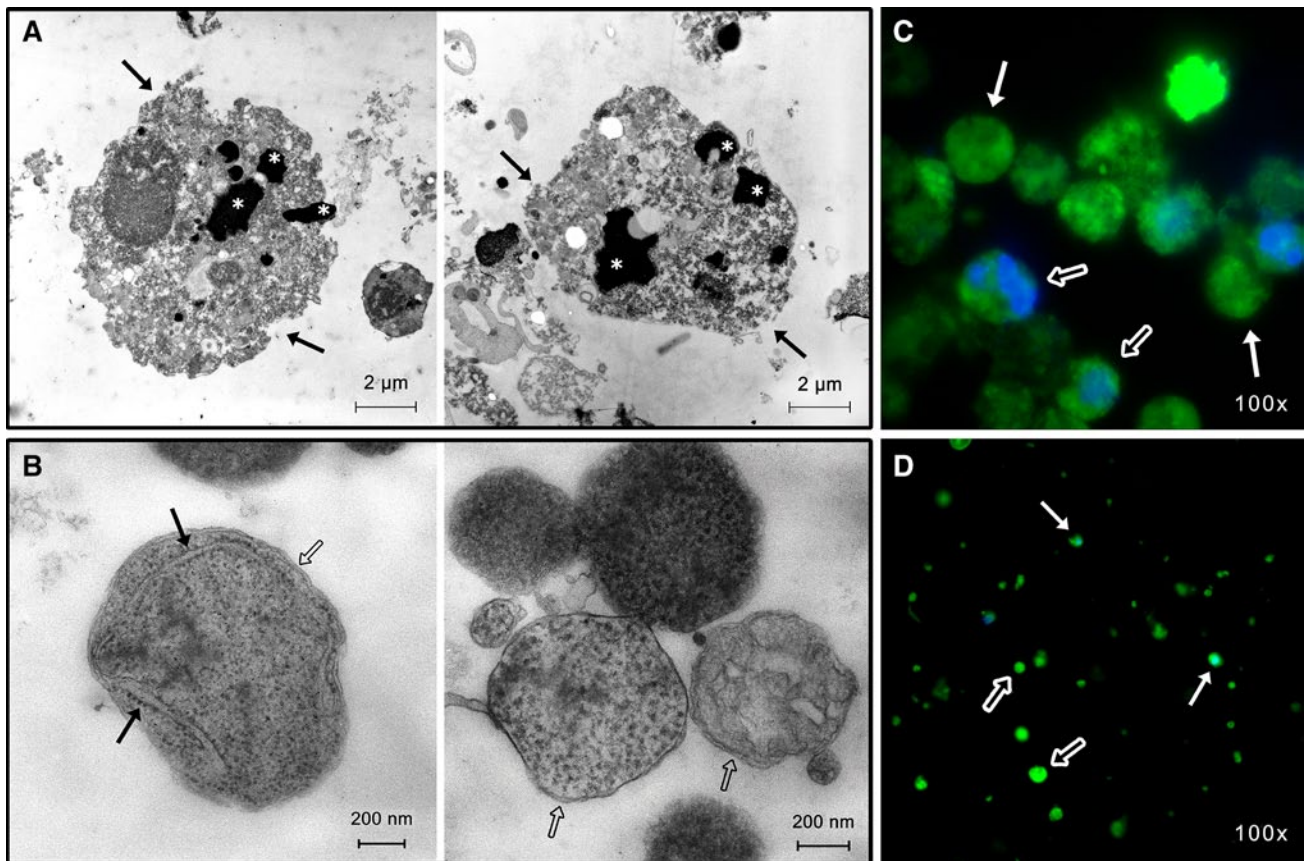
Fig. 1 Analysis of isolated apoptotic fractions. **a** and **b** Transmission electron microscopic analysis of isolated ACR (**a**) and blebs (**b**). The isolated ACR fraction contained large cellular bodies of 4–10 μm in diameter, of which the membrane appeared to be locally disintegrated (**a**, *arrows*). Electron dense areas reside within the ACR (**a**, *asterisks*) that are enclosed by a membrane and represent the latest stages of chromatin translocation to the periphery of the cell. The bleb fraction contains a heterogeneous population of vesicles which are 0.2–0.6 μm in diameter and have a double membrane (**b**, *open arrows*). Structures resembling ER and ribosomes (**b**, *closed arrows*) could be detected in some blebs. **c** and **d** Fluorescence labeling with CFSE (*green*; protein) and Hoechst 33342 (*blue*; DNA) of ACR (**c**) and blebs (**d**) derived from apoptotic HL60 cells. Forty-eight hours after inducing apoptosis using mitoxantrone, most ACR lost all (**c**; *solid arrows*) or most (**c**; *open arrows*) chromatin. The isolated bleb fraction contained mainly vesicles that did not stain positive for Hoechst 33342 (**d**; *open arrows*). Few blebs did enclose detectable amounts of chromatin (**d**; *solid arrows*)

range 26–86 %) (Fig. 2c, immature). These percentages decreased to a mean of 63 % (range 13–92 %) and 35 % (range 6–80 %), respectively, after inducing MoDC maturation (Fig. 2c, maturing). Similar results were obtained when loading MoDC with ACR or blebs derived from HS-induced apoptosis (data not shown). Moreover, the uptake of blebs was significantly increased, whereas there was no significant difference in the uptake of ACR, compared to unseparated apoptotic cells (Fig. 2d). Therefore, subsequent experiments were performed using the separated fractions.

Increased CCR7 expression and migration toward CCL19 by MoDC which have ingested blebs

Next, we determined whether ingestion of mitoxantrone-induced ACR or blebs altered MoDC phenotype. After 48 h of co-culture, we could not detect differences in the expression levels of the tested markers (CD1a, CD14, CD40, CD54, CD80, CD83, and CD86, data not shown), between ACR- or bleb-loaded MoDC, except for the lymph node homing receptor CCR7. CCR7 expression was upregulated on mature MoDC that had ingested either ACR or blebs, compared to unloaded MoDC (Fig. 3a). We observed a reduction in the migration toward the lymph node homing chemokine CCL19 (Mip-3β; CCR7 ligand), after loading with either ACR or blebs (18 vs. 5.5 % ($p = 0.009$) and 9.3 % ($p = 0.03$), respectively; data not shown). However, MoDC that had ingested blebs were more potent in migrating toward CCL19, as compared to those that had taken up ACR; a mean of 14 % (range 2–35 %) of MoDC that had ingested blebs were able to migrate toward CCL19, as compared to only 5 % (range 1–16 %) of MoDC that had ingested ACR (Fig. 3b).
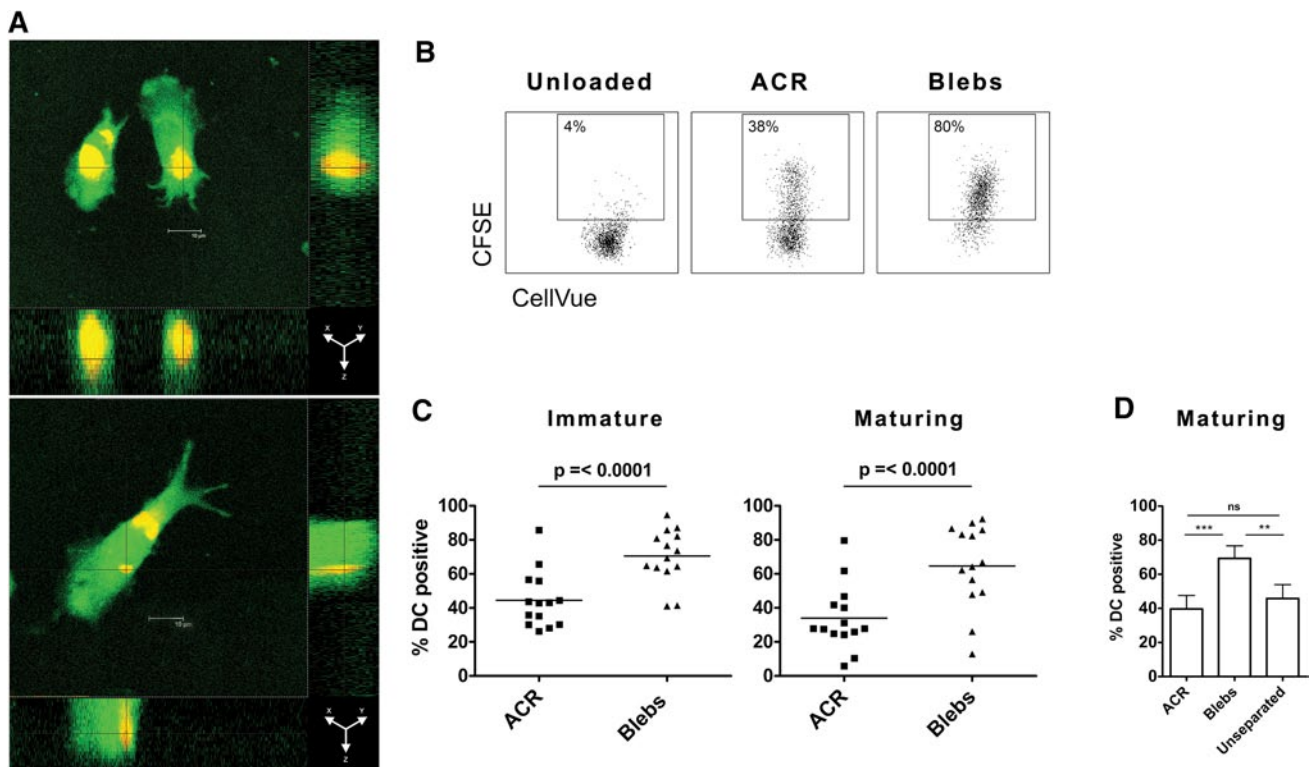
Fig. 2 Uptake of apoptotic material by MoDC. **a** CFSE-labeled MoDC (*green*) were loaded with either PKH26-labeled ACR or blebs (*red*) and analyzed using confocal microscopy. Both ACR (**a**, *top panel*) and blebs (**a**, *lower panel*) are internalized by MoDC (*yellow*), as visualized by the enclosure of both apoptotic fractions by MoDC in *X*, *Y*, and *Z* directions. Optical magnification ×42 and ×3.5 digital zoom. **b** Representative flow cytometric analysis of the uptake quan-
tification of the apoptotic fractions by MoDC. **c** Uptake by immature and maturing MoDC of blebs and ACR ($n = 14$). **d** The percentage ingestion of isolated ACR and blebs, as compared to the unseparated apoptotic cell preparation, by maturing MoDC ($n = 5$). Shown are the mean values and the standard error of the mean (SEM). ******$p = 0.003$; *******$p = 0.0002$
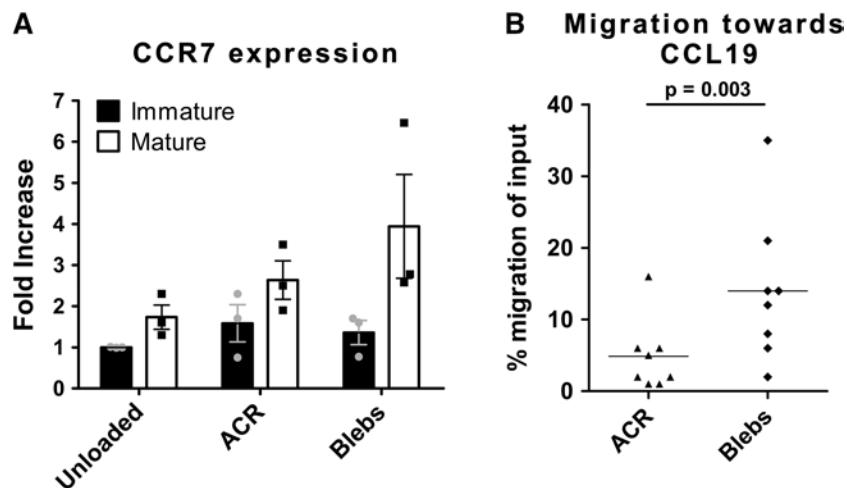

Fig. 3 CCR7 expression on (loaded) MoDC and subsequent migration toward CCL19. **a** Whereas no difference in expression of the lymph node homing chemokine receptor CCR7 could be detected in immature MoDC (*black bars* and *circles* as individual experiments), loading of mature MoDC (*white bars* and *squares* as individual experiments) with either ACR or blebs led to an increased expression of CCR7. This increase was most pronounced when MoDC were
loaded with blebs ($n = 3$). Shown are the mean values and the SEM. **b** In concordance with an increased expression of CCR7, migration of ACR- or bleb-loaded mature MoDC revealed that MoDC which had ingested blebs were also able to migrate toward CCL19 (Mip-3β) to a higher degree (14 %; range 2–35 %) in a transwell migration assay, compared to ACR (5 %; range 1–16 %) ($p = 0.003$, $n = 8$)
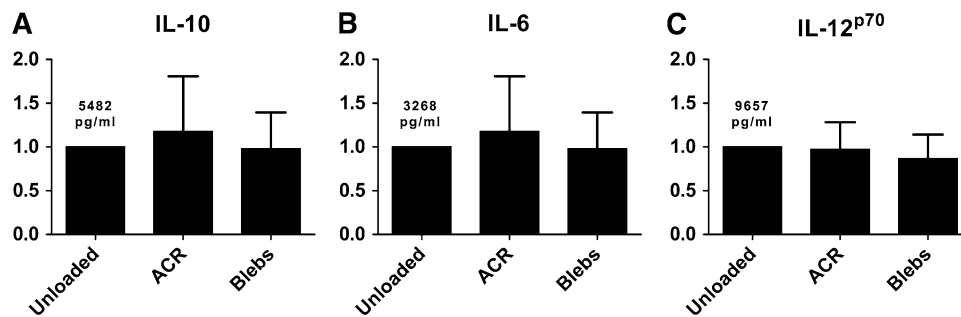
Fig. 4 Cytokine production by (loaded) MoDC after CD40 ligation. **a–c** Cytokine production by unloaded, ACR-, or bleb-loaded immature MoDC after CD40 ligation. Supernatants were analyzed after overnight incubation in the presence of 1,000 U/ml IFNγ. No differences could be detected in the production of the measured cytokines IL-10 (**a**), IL-6 (**b**), or IL-12p70 (**c**). The mean cytokine concentrations of unloaded MoDC are shown and set to one ($n = 3$). Shown are the mean values and the SEM

Unaffected production of pro-inflammatory cytokines by MoDC after ingesting either ACR or blebs

To avoid interference of trace amounts of mitoxantrone with MoDC function (as described in the "Materials and methods" section), we assessed whether ingestion of either HS-derived ACR or blebs induced an altered cytokine profile, as compared to unloaded MoDC. To this end, ACR- or bleb-loaded MoDC were activated by the CD40 ligand expressing cell line J558 in the presence of 1,000 U/ml IFNγ. After overnight incubation, the concentration of the T_H-skewing cytokines IL-6 (T_H17), IL-10 (T_H2), and IL-12p70 (T_H1) was determined in the culture supernatants. No clear differences in the production of either IL-6 (Fig. 4a), IL-10 (Fig. 4b) or IL-12p70 (Fig. 4c) could be detected, when analyzing either unloaded, ACR-, or bleb-loaded MoDC.

Increased IFNγ production by allogeneic T cells after priming with bleb-loaded MoDC

Subsequently, we determined whether the loading of MoDC with either heat shock-derived ACR or blebs led to changes in T cell activation and/or proliferation, by priming allogeneic T cells with differentially loaded MoDC. Loading of immature MoDC with ACR led to a reduction in CD4+ T cell proliferation as compared to unloaded- and bleb-loaded MoDC (Fig. 5a). In contrast, mature MoDC loaded with blebs induced a slight, but significant increase in CD4+ T cell proliferation as compared to unloaded MoDC (Fig. 5a). No significant differences in CD8+ T cell proliferation could be detected between the conditions (Fig. 5b).

Next, we determined whether we could detect differences in T_H skewing by analyzing the cytokines produced by allogeneic T cells that were stimulated by differentially loaded MoDC. No differences could be detected in the production of IL-2, IL-4, IL-6, IL-10, IL17a, or TNFα (data not shown). However, priming of T cells with bleb-loaded MoDC led to an increased release of the Th1 effector cytokine IFNγ as compared to unloaded or ACR-loaded MoDC (Fig. 5c).

Higher frequencies of antigen-specific CD8+ T cells with a higher avidity are primed by bleb-loaded MoDC

Finally, we assessed the priming of antigen-specific CD8+ T cells with MoDC loaded with HS-derived ACR or blebs. The apoptotic cell fractions were isolated from HLA-A2-negative HL60 AML cells, transduced with the MART-1 model tumor antigen, in order to prevent direct antigen presentation of the apoptotic cell fractions to T cells. As such, outgrowth of antigen-specific T cells must be the result of cross-priming by loaded (HLA-A2-positive) MoDC. Priming experiments were initiated in 4 healthy donors, with 6–8 wells per donor, and 3–5 restimulation cycles were performed with freshly loaded MoDC. Before each restimulation, the percentage of MART-1$_{26-35L}$-positive CD8+ T cells was analyzed. Priming CD8+ T cells with differentially (i.e., with ACR or blebs) loaded MoDC led to an expansion of MART-1$_{26-35L}$-specific CD8+ T cells in both experimental conditions (Fig. 6a). However, the maximum percentage of MART-1$_{26-35L}$-positive CD8+ T cells differed dramatically, with 1.01 (mean 0.16 %, range 0.05–1.01 %) versus 11.66 % (mean 0.63 %, range 0.04–11.66 %) of CD8+ T cells primed by ACR- or bleb-loaded MoDC, respectively, as summarized in Fig. 6b. After sorting and polyclonal expansion, we analyzed the cytolytic capacity of the primed MART-1-specific CD8+ effector T cells, by co-culturing them with Mel AKR (HLA-A2+MART-1+-positive target) or with HLA-A2+MART− JY or HLA-A2−MART-1+ K562-M (negative control) target cells. MART-1$_{26-35L}$ CD8+ T cells primed by either ACR- or bleb-loaded MoDC were capable of lysing Mel AKR at similar rates (Fig. 6c).

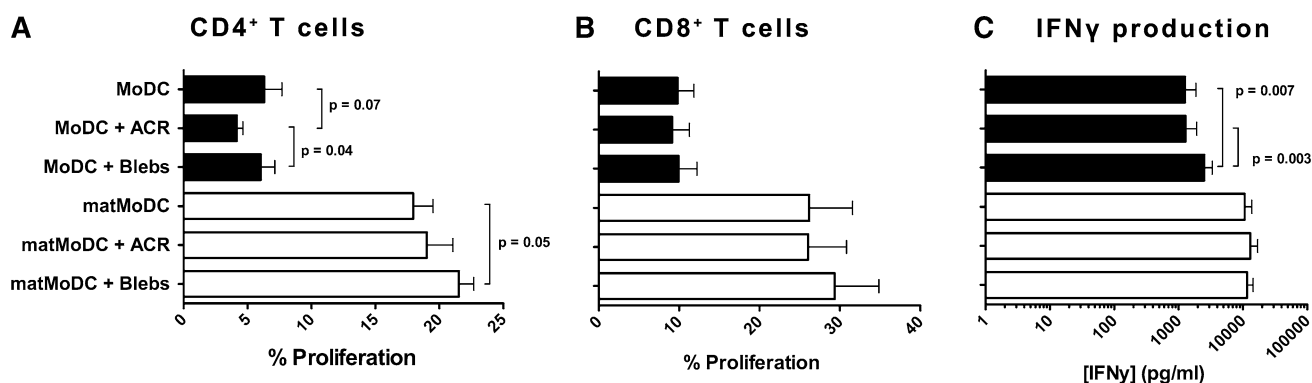**A** CD4⁺ T cells   **B** CD8⁺ T cells   **C** IFNγ production

Fig. 5 Allogeneic mixed lymphocyte reaction with (loaded) MoDC. **a** and **b** CFSE-labeled, CD14-negative, peripheral blood lymphocytes were cultured with MoDC or MoDC loaded with either heat shock-induced ACR or blebs for 6 days, after which the CFSE dilution was analyzed using flow cytometry, as a measure for T cell proliferation. **a** The proliferation of CD4⁺ T cells stimulated with ACR-loaded immature MoDC was diminished compared to unloaded ($p = 0.07$) and bleb-loaded immature MoDC ($p = 0.04$). Moreover, bleb-loaded mature MoDC induced a significant increase in proliferation of CD4⁺ T cells, as compared to unloaded MoDC ($p = 0.05$, $n = 7$). Statistically significant and relevant p values are shown. **b** No significant differences could be detected in CD8⁺ T cell proliferation, between the different loading strategies ($n = 7$). **c** Peripheral blood lymphocytes were stimulated with (loaded) MoDC for 6 days, after which the cytokine production was determined in the supernatant. Of the cytokines tested (IL-2, IL-4, IL-6, IL-10, TNFα, IFNγ, and IL-17a), only IFNγ production was significantly altered when T cells were stimulated with bleb-loaded immature MoDC, leading to the production of approximately twofold higher levels of IFNγ (2,516 pg/ml), as compared to both unloaded (1,270 pg/ml) and ACR-loaded immature MoDC (1,290 pg/ml; $n = 4$). This difference was overruled by inducing additional maturation (*white bars*). All *bar graphs* represent the mean value and the SEM

Interestingly, analysis of functional T cell avidity by peptide titration followed by IFNγ release read-out showed that MART-1$_{26-35L}$ CD8⁺ T cells primed with bleb-loaded MoDC were able to recognize HLA class I:peptide complexes loaded with peptide concentrations two orders of magnitude lower as compared to CD8⁺ T cells primed by ACR-loaded MoDC (i.e., 12-fold and 107-fold, see Fig. 6d).

Discussion

Broadening the repertoire of LAA presented by MoDC is likely to increase the efficacy of DC vaccination. However, only a limited number of LAA have been characterized to date, and even fewer can be used in a patient-specific setting. Moreover, patient-specific frame-shift mutations are described to play a role in anti-tumor immunity [30], most of which are yet to be defined. The use of whole-tumor cell vaccines circumvents the need for LAA characterization and HLA matching and furthermore broadens the array of presented LAA as well as facilitating personalized immunotherapy.

The finding that apoptotic blebs, in contrast to ACR, can induce maturation of bone marrow-derived DC in mice [23, 31] led us to investigate the possibility of using blebs as source of LAA for DC loading in the context of a vaccination strategy. In the current study, we show that blebs, as compared to ACR, derived from apoptotic AML cells, were ingested more efficiently by MoDC. It remains to be determined whether this increase was induced by (1) an enrichment of eat-me signals (e.g., phosphitadyl serine and calreticulin) on the surface of blebs, (2) a different mechanism of ingestion (phagocytosis vs. receptor-mediated endocytosis or fusion), or (3) whether the increased uptake was solely based on spatial considerations as a result of the approximately tenfold size difference between ACR and blebs. In the current study, we used the HL60 AML cell line (and equivalent data were obtained for the K562 CML cell line; data not shown); future studies should also explore the use of primary AML blasts in an autologous setting.

One of the hurdles in effective DC vaccination is the limited migration of (intradermally) injected DC from the site of injection toward the afferent lymph node [32]. Although not significant, we observed a trend toward increased CCR7 expression after loading, which was especially evident after loading with blebs and subsequent MoDC maturation. This could be a result of the presence of danger-associated molecular patterns [33] that could potentially have an additive effect following cytokine-induced maturation. Importantly, the observed increase in migration toward CCL19 of MoDC after taking up blebs is clearly favorable in this regard. Apart from CCR7 expression, neither ingestion of ACR nor of blebs resulted in clear alterations in phenotype, nor in cytokine production of MoDC. Contradictory data have been published on the effects of apoptotic cells on DC maturation. Presentation of self-antigens by DC under non-inflammatory conditions has been shown to induce self-tolerance [13]. Moreover, ingestion of apoptotic cells by DC inhibits NFκB
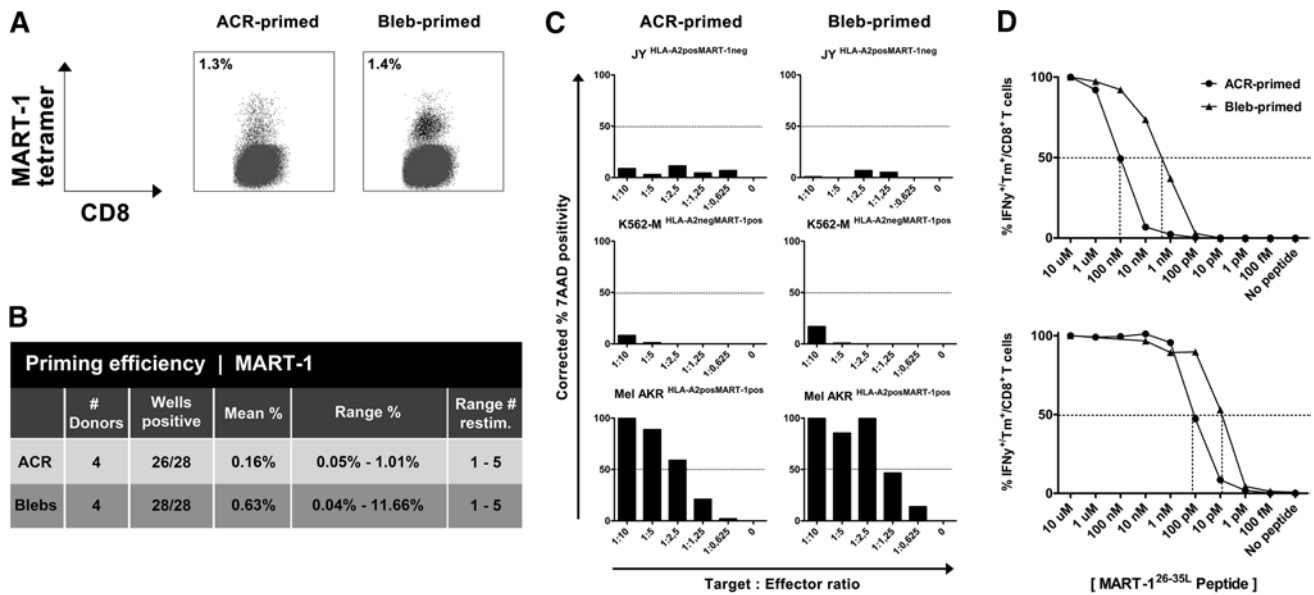
Fig. 6 CD8+ T cell cross-priming, cytotoxicity, and avidity. **a** Priming of CD8+ T cells (gated on FCS/SSC, 7AAD−, CD3+, and CD8+) with heat shock-induced ACR- or bleb-loaded MoDC led to an expansion of MART-1$_{26-35L}$-specific CD8+ T cells, as measured by tetramer staining. No tetramer positivity was observed when CD8+ T cells were primed with unloaded MoDC (data not shown). **b** A total of 4 priming experiments with CD8+ T cells and autologous MoDC from healthy donors were performed. Four to six wells were initiated per donor, and the percentage of MART-1$_{26-35L}$-positive CD8+ T cells was assessed before each restimulation (3–5 restimulations per donor). Positive wells were defined as >0.03 % and >15 Tm+ events or >20 Tm+ events in two subsequent measurements, and the maximum percentage positivity of each well was determined within each priming experiment. The mean percentage of expanded MART-1$_{26-35L}$ CD8+ T cells that were primed with ACR-loaded MoDC was 0.16 % (range 0.05–1.01 %), as compared to 0.63 % (range 0.04–11.66 %) when primed with bleb-loaded MoDC. **c** Co-culture of sorted and expanded MART-1$_{26-35L}$-specific CD8+ T cells at increasing effector-to-target ratios with JY, or K562-M target cells, did not result in an increase in cytotoxicity, as measured by 7AAD-positive target cells (**c** *top four panels*; representative example of 2 cytotoxicity experiments). However, co-culture with Mel AKR target cells showed an increasing cytotoxicity with increasing number of effector cells, by MART-1$_{26-35L}$-specific CD8+ T cells primed with both ACR- and bleb-loaded MoDC (**c** *lower two panels*). The highest ratio (1:10) was set to 100 %, in order to visualize the IC50 values. Maximum 7AAD positivity of MEL AKR was 80 % and 61 %, when co-cultured with, respectively, ACR-primed or bleb-primed CD8+ T cells. **d** T cell avidity analysis showed that MART-1$_{26-35L}$-specific CD8+ T cells primed with bleb-loaded MoDC (*triangles*) could detect 12-fold and 107-fold lower MART-1$^{26-35}$ peptide concentrations, as compared to those primed with ACR-loaded MoDC (circles; avidity assays from 2 independent successful priming experiments)

activation and induces the production of regulatory cytokines (e.g., IL-10, TGFβ), whereas the production of pro-inflammatory cytokines (e.g., IL-12 and TNFα) is hampered following Toll-like receptor ligation [14–18]. The expression of co-stimulatory molecules and T cell stimulatory capacity by apoptotic cell-loaded DC is diminished compared to unloaded DC [34–36]. In contrast, apoptotic cell-loaded DC have also been shown to induce T cell responses [37, 38]. The contradictory data on apoptotic cell loading strategies for DC vaccination purposes could be a result of either the method of apoptosis induction or the method of isolation after induction with different bleb:ACR contents of the resulting product. Moreover, discrepancies observed after administration of apoptotic cells in murine models could be a result of the ingestion by different phagocytes (DC vs. macrophages and non-professional phagocytes).

In contrast to dampening MoDC function and T cell activation, both ACR and bleb-loaded MoDC were able to stimulate T cells, although loading MoDC with ACR, without the induction of DC maturation (using IL-1β, IL-6, PGE-2, and TNF-α), did diminish CD4+ T cell proliferation compared to unloaded or bleb-loaded MoDC. Importantly, co-culture of PBL with bleb-loaded (immature) MoDC led to T$_H$1 skewing, based on the significantly higher levels of IFNγ production, compared to unloaded and ACR-loaded MoDC. Our data are in keeping with data obtained by Fransen et al. [23], although we could not detect an increase in IL-17 production by PBL after stimulation with bleb-loaded MoDC (data not shown). This lack of IL-17 production in a MLR could be a result of (1) species difference, (2) the origin of the DC used (MoDC vs. BMDC), or (3) the responder cells used in the MLR (PBL vs. splenocytes) and does not exclude the induction of IL-17 producing T cells in vivo.

We observed a higher percentage of MART-1$_{26-35L}$-specific CD8+ T cells when primed with bleb-loaded MoDC in the conducted priming experiments, which can be explained by multiple factors. For instance, the increase in uptake of

blebs by MoDC could lead to an increased antigen load per MoDC, by which these MoDC are able to present LAA in a greater number of HLA class I molecules, or for a prolonged period of time. Also, blebs could contain more readily processable sources of antigen, e.g., defective ribosomal products (DRIPs), rapidly degradable poly-peptides, and translated proteins, due to the presence of the ER. These antigen sources have been described to lead to very efficient presentation in the context of HLA class I and are essential sources of presented antigen during viral infections [39, 40]. Whether the presence of these peptides in blebs is elevated remains to be elucidated, but DRIPs within autophagosomes have been reported to be efficiently cross-presented [41]. Combined with the efficient uptake, this could render blebs a more effective source of LAA compared to ACR.

Our observation that bleb-loaded MoDC prime CD8$^+$ T cells of higher avidity compared to ACR-loaded MoDC is likely to be an effect of the ingested blebs on the functionality of the MoDC, rather than differences in processing and presentation efficiency of the antigen. As we found no differences in, e.g., release of IL-12p70 or other T cell stimulatory cytokines or expression levels of co-stimulatory molecules, the underlying mechanism in this regard as yet remains obscure. Nevertheless, this impressive difference in functional avidity clearly indicates a preferred use of blebs over ACR for immunotherapeutic purposes.

In conclusion, we have shown that ingestion of human apoptotic blebs derived from the AML cell line HL60 can induce lymph node migration capacity in MoDC as well as the ability to prime IFNγ producing effector T cells and high-avidity tumor reactive CTL. Using bleb-loaded MoDC for the induction of tumor-directed cytotoxic T cell responses could therefore be a potent novel strategy for treating AML patients.

References

1. Banchereau J, Palucka K (2005) Dendritic cells as therapeutic vaccines against cancer. Nat Rev Immunol 5:296–306. doi:10.1038/nri1592

2. Steinman RM, Banchereau J (2007) Taking dendritic cells into medicine. Nature 449:419–426. doi:10.1038/nature06175

3. Westers TM, Stam AGM, Scheper RJ et al (2003) Rapid generation of antigen-presenting cells from leukaemic blasts in acute myeloid leukaemia. Cancer Immunol Immunother 52:17–27. doi:10.1007/s00262-002-0316-0

4. Westers TM, Van Den Ancker W, Bontkes HJ et al (2011) Chronic myeloid leukemia lysate-loaded dendritic cells induce T-cell responses towards leukemia progenitor cells. Immunotherapy 3:569–576

5. Nestle FO, Alijagic S, Gilliet M et al (1998) Vaccination of melanoma patients with peptide- or tumor lysate-pulsed dendritic cells. Nat Med 4:328–332

6. Thurner B, Haendle I, Röder C et al (1999) Vaccination with mage-3A1 peptide-pulsed mature, monocyte-derived dendritic cells expands specific cytotoxic T cells and induces regression of some metastases in advanced stage IV melanoma. J Exp Med 190:1669–1678

7. Van Tendeloo VF, Van de Velde A, Van Driessche A et al (2010) Induction of complete and molecular remissions in acute myeloid leukemia by Wilms' tumor 1 antigen-targeted dendritic cell vaccination. Proc Natl Acad Sci USA 107:13824–13829. doi:10.1073/pnas.1008051107

8. Boczkowski D, Nair SK, Snyder D, Gilboa E (1996) Dendritic cells pulsed with RNA are potent antigen-presenting cells in vitro and in vivo. J Exp Med 184:465–472

9. Bontkes HJ, Kramer D, Ruizendaal JJ et al (2007) Dendritic cells transfected with interleukin-12 and tumor-associated antigen messenger RNA induce high avidity cytotoxic T cells. Gene Ther 14:366–375

10. Willemijn VDA, Van Luijn MM, Westers TM et al (2010) Recent advances in antigen-loaded dendritic cell-based strategies for treatment of minimal residual disease in acute myeloid leukemia. Immunotherapy 2:69–83

11. Van den Ancker W, van Luijn MM, Ruben JM et al (2011) Targeting Toll-like receptor 7/8 enhances uptake of apoptotic leukemic cells by monocyte-derived dendritic cells but interferes with subsequent cytokine-induced maturation. Cancer Immunol Immunother 60:37–47. doi:10.1007/s00262-010-0917-y

12. Kitawaki T, Kadowaki N, Fukunaga K et al (2011) Cross-priming of CD8(+) T cells in vivo by dendritic cells pulsed with autologous apoptotic leukemic cells in immunotherapy for elderly patients with acute myeloid leukemia. Exp Hematol 39(424–433):e2. doi:10.1016/j.exphem.2011.01.001

13. Liu K, Iyoda T, Saternus M et al (2002) Immune tolerance after delivery of dying cells to dendritic cells in situ. J Exp Med 196:1091–1097. doi:10.1084/jem.20021215

14. Morelli AE (2006) The immune regulatory effect of apoptotic cells and exosomes on dendritic cells: its impact on transplantation. Am J Transplant 6:254–261. doi:10.1111/j.1600-6143.2005.01197.x

15. Municio C, Hugo E, Alvarez Y et al (2011) Apoptotic cells enhance IL-10 and reduce IL-23 production in human dendritic cells treated with zymosan. Mol Immunol 1–10. doi:10.1016/j.molimm.2011.07.022

16. Ren G, Su J, Zhao X et al (2008) Apoptotic cells induce immunosuppression through dendritic cells: critical roles of IFN-gamma and nitric oxide. J Immunol 181:3277–3284

17. Sen P, Wallet MA, Yi Z et al (2007) Apoptotic cells induce Mer tyrosine kinase-dependent blockade of NF-κB activation in dendritic cells. Blood 109:653–660. doi:10.1182/blood-2006-04-017368

18. Stuart LM, Lucas M, Simpson C et al (2002) Inhibitory effects of apoptotic cell ingestion upon endotoxin-driven myeloid dendritic cell maturation. J Immunol 168:1627–1635

19. Lomonosova E, Chinnadurai G (2008) BH3-only proteins in apoptosis and beyond: an overview. Oncogene 27(Suppl 1):S2–S19

20. Franz S, Herrmann K, Fürnrohr BG et al (2007) After shrinkage apoptotic cells expose internal membrane-derived epitopes on their plasma membranes. Cell Death Differ 14:733–742. doi:10.1038/sj.cdd.4402066

21. Lane JD, Allan VJ, Woodman PG (2005) Active relocation of chromatin and endoplasmic reticulum into blebs in late apoptotic cells. J Cell Sci 118:4059–4071. doi:10.1242/jcs.02529

22. Meesmann HM, Fehr E-M, Kierschke S et al (2010) Decrease of sialic acid residues as an eat-me signal on the surface of apoptotic lymphocytes. J Cell Sci 123:3347–3356

23. Fransen JH, Hilbrands LB, Ruben J et al (2009) Mouse dendritic cells matured by ingestion of apoptotic blebs induce T cells to produce interleukin-17. Arthritis Rheum 60:2304–2313. doi:10.1002/art.24719

24. Suber T, Rosen A (2009) Apoptotic cell blebs: repositories of autoantigens and contributors to immune context. Arthritis Rheum 60:2216–2219. doi:10.1002/art.24715

25. Wlodkowic D, Skommer J, Pelkonen J (2007) Towards an understanding of apoptosis detection by SYTO dyes. Cytom Part A J Int Soc Anal Cytol 71:61–72. doi: 10.1002/cyto.a.20366

26. Liu Y, Qureshi M, Xiang J (2002) Antitumor immune responses derived from transgenic expression of CD40 ligand in myeloma cells. Cancer Biother Radiopharm 17:11–18. doi:10.1089/10849780252824028

27. Schreurs MWJ, Scholten KBJ, Kueter EWM et al (2003) In vitro generation and life span extension of human papillomavirus type 16-specific, healthy donor-derived CTL clones. J Immunol 171:2912–2921

28. Hooijberg E, Ruizendaal JJ, Snijders PJ et al (2000) Immortalization of human CD8+ T cell clones by ectopic expression of telomerase reverse transcriptase. J Immunol 165:4239–4245

29. Mathivanan S, Ji H, Simpson RJ (2010) Exosomes: extracellular organelles important in intercellular communication. J Proteomics 73:1907–1920. doi:10.1016/j.jprot.2010.06.006

30. Fischer E, Kobold S, Kleber S et al (2010) Cryptic epitopes induce high-titer humoral immune response in patients with cancer. J Immunol 185:3095–3102

31. Fransen JH, Hilbrands LB, Jacobs CW et al (2009) Both early and late apoptotic blebs are taken up by DC and induce IL-6 production. Autoimmunity 42:325–327

32. Verdijk P, Aarntzen EHJG, Lesterhuis WJ et al (2009) Limited amounts of dendritic cells migrate into the T-cell area of lymph nodes but have high immune activating potential in melanoma patients. Clin Cancer Res 15:2531–2540. doi:10.1158/1078-0432.CCR-08-2729

33. Wickman GR, Julian L, Mardilovich K et al (2013) Blebs produced by actin-myosin contraction during apoptosis release damage-associated molecular pattern proteins before secondary necrosis occurs. Cell Death Differ. doi:10.1038/cdd.2013.69

34. Gallucci S, Lolkema M, Matzinger P (1999) Natural adjuvants: endogenous activators of dendritic cells. Nat Med 5:1249–1255. doi:10.1038/15200

35. Herr W, Ranieri E, Olson W et al (2000) Mature dendritic cells pulsed with freeze-thaw cell lysates define an effective in vitro vaccine designed to elicit EBV-specific CD4(+) and CD8(+) T lymphocyte responses. Blood 96:1857–1864

36. Schnurr M, Galambos P, Scholz C et al (2001) Tumor cell lysate-pulsed human dendritic cells induce a T-cell response against pancreatic carcinoma cells: an in vitro model for the assessment of tumor vaccines. Cancer Res 61(17):6445–6450

37. Kokhaei P, Rezvany MR, Virving L et al (2003) Dendritic cells loaded with apoptotic tumour cells induce a stronger T-cell response than dendritic cell-tumour hybrids in B-CLL. Leukemia 17:894–899. doi:10.1038/sj.leu.2402913

38. Wieckowski E, Chatta GS, Mailliard RM et al (2011) Type-1 polarized dendritic cells loaded with apoptotic prostate cancer cells are potent inducers of CD8(+) T cells against prostate cancer cells and defined prostate cancer-specific epitopes. Prostate 71:125–133. doi:10.1002/pros.21228

39. Dolan BP, Li L, Takeda K et al (2010) Defective ribosomal products are the major source of antigenic peptides endogenously generated from influenza A virus neuraminidase. J Immunol 184:1419–1424

40. Yewdell JW, Nicchitta CV (2006) The DRiP hypothesis decennial: support, controversy, refinement and extension. Trends Immunol 27:368–373. doi:10.1016/j.it.2006.06.008

41. Li Y, Wang L-X, Pang P et al (2011) Tumor-derived autophagosome vaccine: mechanism of cross-presentation and therapeutic efficacy. Clin Cancer Res 17:7047–7057. doi:10.1158/1078-0432.CCR-11-0951